World Applied Sciences Journal 8 (10): 1234-1239, 2010
ISSN 1818-4952
© IDOSI Publications, 2010

Effects of Incidence Angle on Nanoscale Radiative Properties of Doped Silicon Multilayer Structures

S.A.A. Oloomi, A. Saboonchi and A. Sedaghat

Department of Mechanical Engineering, Isfahan University of Technology,
Isfahan, 84156-83111, I.R. of Iran

Abstract: This work uses transfer-matrix method for calculating the radiative properties. Doped silicon is used and Coherent Formulation is applied. The considered wavelengths are 0.5 µm for visible range and 0.9 µm for infrared wavelength. Results showed that in visible wavelength, reflectance increases when incidence angle increases up to 50° and then a little decreasing happens for reflectance till incidence angle reaches 65°. Reflectance increases rapidly for incidence angle between 65° to 89°. In infrared wavelength, reflectance increases smoothly with increasing in incidence angle up to 54° for silicon dioxide coating and then it increases rapidly. But for silicon nitride coating the reflectance decreases with increasing incidence angle up to 54° and then it increases rapidly. In infrared wavelength, Silicon dioxide coating has higher emittance than silicon nitride coating for 0°#2# 17° and 82°#2#89°, but for 18° #2# 81° silicon nitride coating has higher emittance than silicon dioxide coating. Therefore thermal radiaitive properties of nanoscale multilayer structures strongly depend on incidence angle.

PACS Numbers: 68.37.Ef-81.07.-b
Key words: Incidence Angle % Emittance % Reflectance % Doped Silicon and Nanoscale

INTRODUCTION

The radiative properties of semiconductors are important in advancement of some manufacturing technologies such as rapid thermal processing [1]. Since the major heating source in the rapid thermal processing is lamp radiation, the knowledge of radiative properties is important in temperature control during the process. Silicon is the semiconductor that plays a vital role in integrated circuits and MEMS/NEMS [2]. Semitransparent crystalline silicon solar cells can improve the efficiency of solar power generation [3]. Accurate radiometric temperature measurements of silicon wafers and heat transfer analysis of rapid thermal processing furnaces require a thorough understanding of the radiative properties of the silicon wafer, whose surface may be coated with dielectric or absorbing films [1]. In fact, surface modification by coatings can significantly affect the radiative properties of a material [4, 5]. For lightly doped silicon, silicon dioxide coating has higher reflectance than silicon nitride coating for visible wavelengths. In visible wavelengths the reflectance increases as the temperature increases due to decreasing emittance; but in infrared wavelengths, the reflectance and transmittance decrease as the temperature increases [4]. This work uses transfer-matrix method and the coherent formulation for calculating the radiative properties of dopped silicon. The Drude model is used for obtaining the optical constants of doped silicon. In this work, Phosphorus and boron are default impurities for n-type and p-type, respectively.

Modeling

Coherent Formulation: When the thickness of each layer is comparable or less than the wavelength of electromagnetic waves, the wave interference effects inside each layer play an importantrole in accurate prediction of the radiative properties of the multilayer structure of thin films. The transfer-matrix method provides a convenient way to calculate the radiative properties of the multilayer structure of thin films (Figure 1).

Corresponding Author: S.A.A. Oloomi, Department of Mechanical Engineering, Isfahan University of Technology, Isfahan, 84156-83111, I.R. of Iran E.mail: Amiroloomi@me.iut.ac.ir

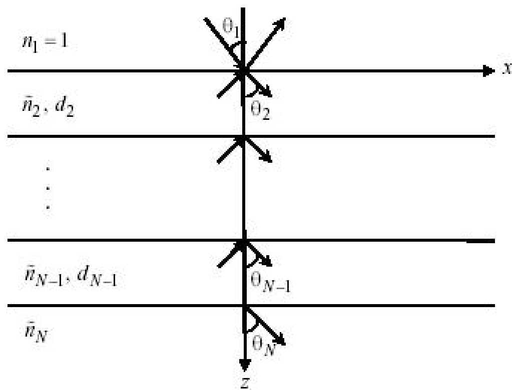

Fig. 1: The geometry for calculating the radiative properties of a multilayer structure

Assuming that the electromagnetic field in the jth medium is a summation of forward and backward waves in the z-direction, the electric field in each layer can be expressed by

$$E_j \begin{cases} \left[A_1 e^{iq1z^z} + B_1 e^{-iq1z^z} \right] e^{(iq_x x - iwt)}, \; j = 1 \\ \left[A_j e^{iq_{jz}(z - z_{j-1})} + B_j e^{-iq_{jz}(z - z_{j-1})} \right] e^{(iq_x x - iwt)}, \; j = 2, 3, ...N \end{cases} \quad (1)$$

here, A_j and B_j are the amplitudes of forward and backward waves in the jth layer. Detailed descriptions of how to solve Eq. (1) for A_j and B_j is given in [5].

Optical Constants

The Refractive Index of Silicon: The Jellison and Modine (J-M) expression of therefractive index for a wavelength between 0.4 µm and 0.84 µm is given in [6]. Li [7] developed a functional relation, for the refractive index of silicon that covers the wavelength region between 1.2 µm and 14 µm. The J-M expression is used in this study to calculate the refractive index of silicon for the wavelength region from 0.5 µm to 0.84 µm but Li's expression is employed for wavelengths above 1.2 µm. For a wavelength range of 0.84 µm to 1.2 µm, we use a weighted average based on the extrapolation of the two expressions.

The Extinction Coefficient of Silicon: The J-M expression of the extinction coefficient, covering the wavelength range from 0.4 µm to 0.84 µm, is given in [6]. The absorption coefficient can be deduced from the extinction coefficient. For longer wavelength regions, Timans suggested that the absorption coefficient can be expressed as a summation of the band gap absorption and free-carrier absorption as in the following [1]:

$$''(8,T) = ''_{BG}(8, T) + ''_{FC}(8, T) \quad (2)$$

The expression for the band gap absorption can be found in the work by MarcFalane *et al*. [8, 9]. For free-carrier absorption, Sturm and Reaves [10] suggested an expression. Vandenabeele and Maex [11] proposed a semi-empirical relation for calculating the extinction coefficient as functions of wavelength and temperature due to free-carrier absorption. The Vandenabeele and Maex (V-M) expression is given by

$$\boldsymbol{a}_{FC}(\boldsymbol{l},T) = 4.15\times10^{-5}\boldsymbol{l}^{1.51}(T+273.15)^{2.95}\exp(\frac{-7000}{T+273.15}) \quad (3)$$

Rogne *et al*. [12] demonstrated that the absorption coefficient calculated from the V-M expression agrees well with experimental data for the wavelength region between 1.0 µm and 9.0 µm at elevated temperatures. The optical constants of silicon dioxide are mainly based on the data collected in Palik [13].

The Drude Model for the Optical Constants of Doped Silicon: The complex dielectric function is related to the refractive index (n) and the extinction coefficient (k) by $g(T)=(n+ik)^2$. To account for doping effects, the Drude model is employed and the dielectric function of both intrinsic and doped silicon is expressed as follows [14]:

$$\boldsymbol{e}(\boldsymbol{w}) = \boldsymbol{e}_{bl} - \frac{N_e e^2 / \boldsymbol{e}_0 m_e^*}{\boldsymbol{w}^2 + i\boldsymbol{w}/\boldsymbol{t}_e} - \frac{N_h e^2 / \boldsymbol{e}_0 m_h^*}{\boldsymbol{w}^2 + i\boldsymbol{w}/\boldsymbol{t}_h} \quad (4)$$

The values for the effective density of states at room temperature are found in [15]. The Fermi-Dirac integral $F_{1/2}$ can be simplified by an exponential and the procedures described in [16] are used to determine the Fermi energy satisfying charge neutrality. The ionization energies of phosphorus and boron values are taken from [17]. The scattering time, J_e or J_h, depends on the collisions of electrons or holes with the lattice (phonons) and the ionized dopant sites (impurities or defects); hence, it generally depends on temperature and dopant concentration. The total scattering time (for the case of J_e), which consists of the above two mechanisms, can be expressed as [17]:

$$\frac{1}{\boldsymbol{t}_e} = \frac{1}{\boldsymbol{t}_{e-l}} + \frac{1}{\boldsymbol{t}_{e-d}} \quad (5)$$

where, J_{e-l} and J_{e-d} denote the electron-lattice and the electron-defect scattering times, respectively. Similarly, J_h can be related to J_{h-l} and J_{h-d}. In addition, the scattering time, J, is also related to mobility, µ, by the following relation:

$$J = m^* \mu/e \quad (6)$$

At room temperature, the total scattering time $\boldsymbol{t}_e^0$ or $\boldsymbol{t}_h^0$, which depends on the dopant concentration, can be determined from the fitted mobility equations [18]:

$$\boldsymbol{m}_e^0 = \frac{1268}{1+(N_D/1.3\times10^{17})^{0.91}} + 92 \quad (7)$$

$$\boldsymbol{m}_h^0 = \frac{447.3}{1+(N_A/1.9\times10^{17})^{0.76}} + 47.7 \quad (8)$$

Where, the superscript 0 indicates values at 300 °K and N_D or N_A is the dopant concentration of the donor (phosphorus, n-type) or the acceptor (boron, p-type) in cmG3. On the other hand, the scattering time from the lattice contribution $\boldsymbol{t}_{e-l}^0$ or $\boldsymbol{t}_{h-l}^0$, are given in [10]. Because of the relative insignificance of impurity scattering at high temperatures, the following formula will be used to calculate the impurity scattering times:

$$\frac{\boldsymbol{t}_{e-d}}{\boldsymbol{t}_{e-d}^0} = \frac{\boldsymbol{t}_{h-d}}{\boldsymbol{t}_{h-d}^0} = \left(\frac{T}{300}\right)^{1.5} \quad (9)$$

In order to obtain a better agreement with the measured near-infrared absorption coefficients for lightly doped silicon [1, 10-12], the expressions for lattice scattering are modified in the present study as follows:

$$\boldsymbol{t}_{e-l} = \boldsymbol{t}_{e-l}^0 (T/300)^{-3.8} \quad (10)$$

$$\boldsymbol{t}_{h-l} = \boldsymbol{t}_{h-l}^0 (T/300)^{-3.6} \quad (11)$$

RESULTS AND DISCUSSION

In Figure 2, radiative properties of lightly doped, 700-µm-thick Si is plotted as a function of angle of incidence for 8 = 0.9 µm and 8 = 2.7 µm, respectively.

As can be seen in above figures, the change in reflectivity with the angle of incidence is very small from 0° to 70°. The reflectivity changes significantly beyond 70° (figure 2.a). The change in emissivity with the angle of incidence is very small from 0° to 70°. The emissivity changes significantly beyond 70° (figure 2.c). This is once again illustrated in figure. 2.c for three specific temperatures. At high temperatures, the emissivity of silicon reaches its intrinsic value of 0.7 and remains independent of wavelength in the 1–20-µm range. At shorter wavelengths, close to the absorption edge of silicon, the transmittance is negligible. However, for 8=2.7 µm, the transmittance becomes significant, as can be seen in figure. 2.b. At high temperatures, transmittance becomes negligible. At low temperatures, the emissivity of silicon is a complex function of wavelength. The calculated results are in good agreement with results of [19].

Now consider the case in which the silicon wafer is coated with thin film on both sides. One time SiO_2 is used as thin film coating and other time Si_3N_4 is used as thin film coating. The thickness of silicon wafer is 500 µm and the Electromagnetic wave incident differs from 0° to 89°. The considered wavelengths are 0.5 µm for visible range and 0.9 µm for infrared wavelength. The thickness of SiO_2 and Si_3N_4 is 400 nm. Doped silicon is used and Coherent Formulation is applied. Some results of this study are shown below in Tables 1 to 2 and Figures 3 to 4.

Table1: Reflectance of silicon wafer coated by thin film on both sides with n-type impurity concentration of 1e18 cmG3, 25°C

Coating Material	Reflectance 2=0° 8=0.5 µm	Reflectance 2=89° 8=0.5 µm	Average Reflectance 8=0.5 µm	Reflectance 2=0° 8=0.9 µm	Reflectance 2=89° 8=0.9 µm	Average Reflectance 8=0.9 µm
SiO_2	0.1935	0.9368	0.3702	0.1832	0.8835	0.3114
Si_3N_4	0.2192	0.8992	0.3642	0.2234	0.9158	0.2304

Table2: Emittance of silicon wafer coated by thin film on both sides with n-type impurity concentration of 1e18 cmG3, 25°C

Coating Material	Emittance 2=0° 8=0.5 µm	Emittance 2=89° 8=0.5 µm	Average Emittance 8=0.5 µm	Emittance 2=0° 8=0.9 µm	Emittance 2=89° 8=0.9 µm	Average Emittance 8=0.9 µm
SiO_2	0.8065	0.0632	0.6298	0.8168	0.1165	0.6886
Si_3N_4	0.7808	0.1008	0.6358	0.7766	0.0843	0.7696

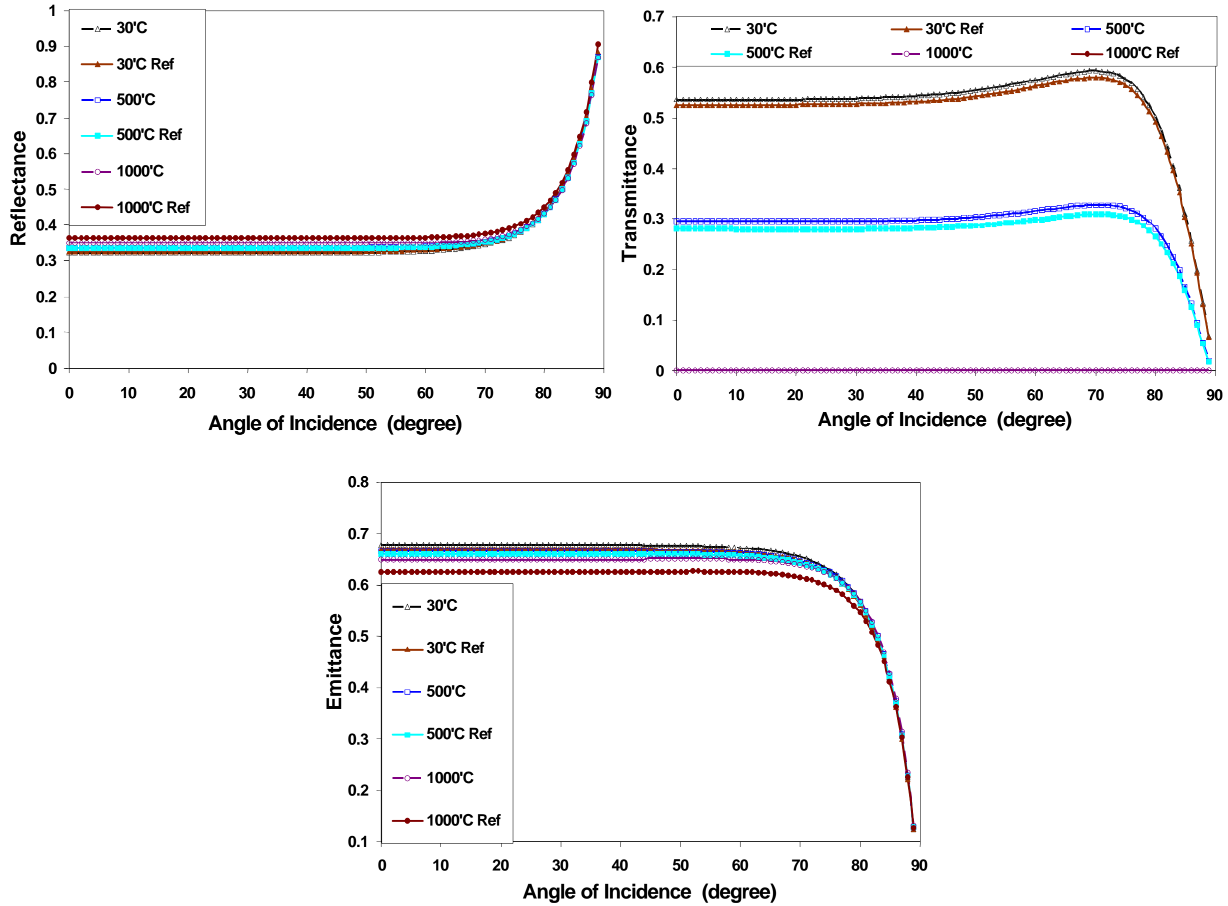

Fig. 2: A comparison of the calculated results with results of [19]

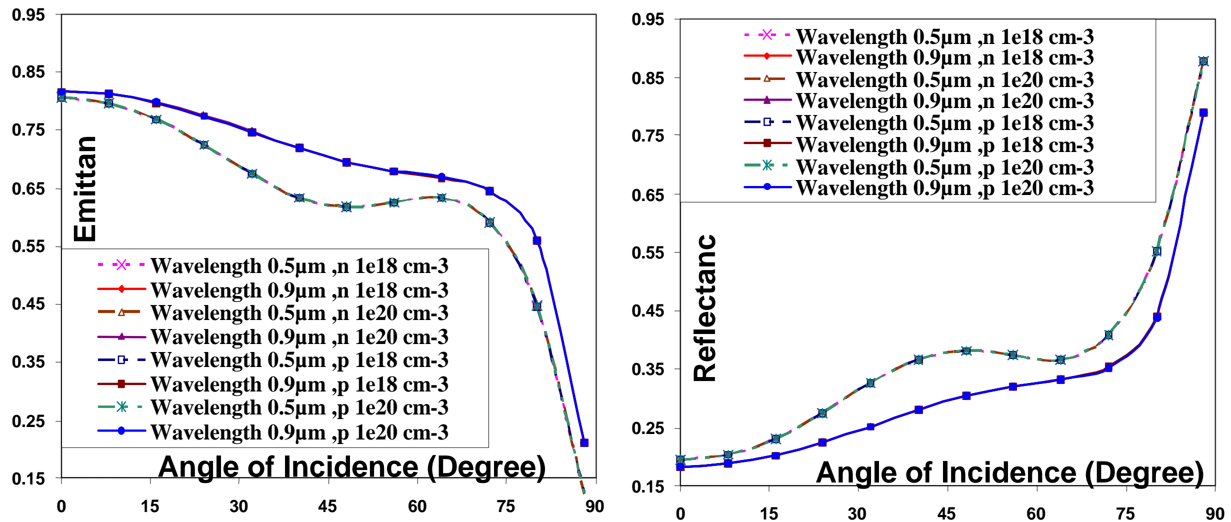

Fig. 3: Emittance and Reflectance of doped silicon wafer coated with a silicon dioxide film on both sides at 25°C

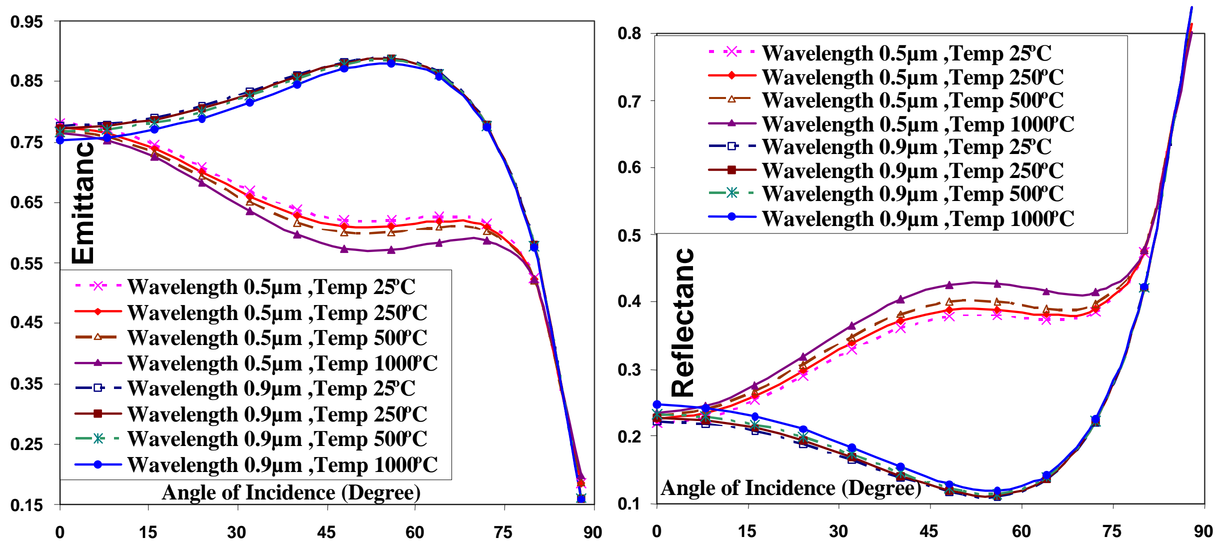

Fig. 4: Emittance and Reflectance of doped silicon wafer coated with a silicon nitride film on both sides with n-type impurity concentration of 1e20 cmG^{3}

CONCLUSION

The effect of wave interference can be understood by plotting the spectral properties such as reflectance or transmittance of a thin dielectric film versus the film thickness and analyzing the oscillations of properties due to constructive and destructive interferences [4].

Results Showed That in Visible Wavelength:

- The Reflectance increases when incidence angle increases up to 50° and then a little decreasing happens for reflectance till incidence angle reaches 65°. Reflectance increases rapidly for incidence angle between 65° to 89°.
- Transmittance is negligible for both thin film coatings.
- Emittance decreases when incidence angle increases up to 50° and then a little increasing happens for emittance till incidence angle reaches 65°. emittance decreases rapidly for incidence angle between 65° to 89°. These behaviors are similar for silicon dioxide coating and silicon nitride coating.
- Results showed that changing in reflectance and emittance vice incidence angle has similar behavior in different temperatures.
- Silicon dioxide coating has higher average reflectance than silicon nitride coating but it has lower average emittance than silicon nitride coating in wavelength 0.5.

Results Showed That in Infrared Wavelength:

- The reflectance increases smoothly with increasing in incidence angle up to 54° for silicon dioxide coating and then it increases rapidly. But for silicon nitride coating the reflectance decreases with increasing incidence angle up to 54° and then it increases rapidly. Therefore thermal radiaitive properties of nanoscale multilayer structures strongly depend on incidence angle.
- In infrared wavelength? emittance decreases smoothly with increasing in incidence angle up to 54° for silicon dioxide coating and then it decreases rapidly. But for silicon nitride coating, the emittance increases with increasing incidence angle up to 54° and then it decreases rapidly. In infrared wavelength, Silicon dioxide coating has higher emittance than silicon nitride coating for 0°#2#17° and 82°#2#89°, but for 18°#2#81° silicon nitride coating has higher emittance than silicon oxide coating.
- Silicon dioxide coating has higher reflectance than silicon nitride coating for 18°#2#81° but for 0°#2#17° and 82°#2#89° silicon nitride coating has higher reflectance than silicon oxide coating.

Results Also Showed That:

- For silicon wafer coated by silicon oxide with n-type impurity concentration of 1e18, average reflectance in 0.5 µm wavelengths is 0.3702 but it is 0.3114 in 0.9 µm

wavelengths. Visible wavelength has higher reflectance than infrared wavelength at room temperature.

- For silicon wafer coated by silicon oxide with n-type impurity concentration of 1e18, average emittance in 0.5 µm wavelengths is 0.6298 but it is 0.6886 in 0.9 µm wavelengths.
- For silicon nitride coating, average emittance in 0.5 µm wavelengths is 0.6358 but it is 0.7696 in 0.9 µm wavelengths. Infrared wavelength has higher emittance than visible wavelength at room temperature.

REFERENCES

1. Timans, P.J., 1996. The Thermal Radiative Properties of Semiconductors, *Advances in Rapid Thermal and Integrated Processing*, Academic Publishers, Dordrecht, Netherlands, pp: 35-102.
2. Fath, P., H. Nussbaumer and R. Burkhardt, 2002. “Industrial Manufacturing of Semitransparent Crystalline Silicon Power Solar Cells”. Sol Energy Mater Sol Cells, l(74): 127–31.
3. Makino, T., 2002. “Thermal Radiation Spectroscopy for Heat Transfer Science and for Engineering Surface Diagnosis”, In: Taine J editor. Heat transfer, 1. Oxford: Elsevier Science, pp: 55-66.
4. Oloomi, S.A.A., A. Sabounchi and A. Sedaghat, 2009. “Computing Thermal Radiative Properties of Nanoscale Multilayer”, “World Academy of Science, Engineering and Technol.,” 37: 929-934.
5. Zhang, Z.M., C.J. Fu and Q.Z. Zhu, 2003. “Optical and Thermal Radiative Properties of Semiconductors Related to Micro/Nanotechnology,” Advanced in Heat Transfer, 37: 179-296.
6. Jellison, G.E. and F.A. Modine, 1994. “Optical Functions of Silicon at Elevated Temperatures,” J. Appl. Phys., 76: 3758-3761.
7. Li, H.H., 1980. “Refractive Index of Silicon and Germanium and Its Wavelength and Temperature Derivatives,” J. Phys. Chem. Ref. Data, 9: 561-658.
8. Macfarlane, G.G., T.P. Mclean, J.E. Quarrington and V. Roberts, 1958. "Fine Structure in the Absorption-Edge Spectrum of Si," Phys. Rev., 111: 1245-1254.
9. Timans, P.J., 1993. "Emissivity of Silicon at Elevated Temperatures," J. Appl. Phys., 74: 6353-6364.
10. Sturm, J.C. and C.M. Reaves, 1992. "Silicon Temperature-Measurement by Infrared Absorption Fundamental Processes and Doping Effects," IEEE Trans. Electron Devices, 39: 81-88.
11. Vandenabeele, P. and K. Maex, 1992. "Influence of Temperature and Backside Roughness on the Emissivity of Si Wafers during Rapid Thermal-Processing," J. Appl. Phys., 72: 5867-5875.
12. Rogne, H., P.J. Timans and H. Ahmed, 1996. "Infrared Absorption in Silicon at Elevated Temperatures," Appl. Phys. Lett., 69: 2190-2192.
13. Palik, E.D., 1998. “Silicon Dioxide (SiO2)”, Handbook of Optical Constants of Solids, San Diego, CA., pp: 749-763.
14. Hebb, J.P., 1997. "Pattern Effects in Rapid Thermal Processing,” Cambridge, MA.
15. Sze, S.M., 2002. Semiconductor Devices, Physics and Technology, 2nd Ed, Wiley, New York.
16. Sze, S.M., 1981. Physics of Semiconductor Devices, 2nd Ed, Wiley, New York.
17. Beadle, W.E., J.C.C. Tsai and R.D. Plummer, 1985. Quick Reference Manual for Silicon Integrated Circuit Technology, Wiley, New York.
18. Morin, F.J. and J.P. Maita, 1954. "Electrical Properties of Silicon Containing Arsenic and Boron," Phys. Rev., 96: 28-35.
19. Ravindra, N.M., *et al.*, 2003. “Modeling and Simulation of Emissivity of Silicon-Related Materials and Structures”, J. Electronic Materials, 32(10): 1052-1058.